CHEMISTRY OF MATERIALS

ARTICLE

pubs.acs.org/cm

Magnetic and Crystallographic Studies of Mg-Herbertsmithite, γ-$Cu_3Mg(OH)_6Cl_2$—A New $S = 1/2$ Kagome Magnet and Candidate Spin Liquid

R. H. Colman,[†] A. Sinclair,[†,‡] and A. S. Wills*[,†]

[†]University College London, Department of Chemistry, 20 Gordon Street, London WC1H 0AJ

Supporting Information

ABSTRACT: Studies are presented of the synthesis, crystal structure, and magnetic properties of the new quantum kagome magnet Mg-herbertsmithite, γ-$Cu_3Mg(OH)_6Cl_2$. The material features strong antiferromagnetic exchange characterized by a Weiss temperature of $\theta_W \simeq -284$ K and a gradual buildup of short-ranged antiferromagnetic correlations upon cooling. No magnetic transition is observed until $T_C \simeq 4-5$ K when a small ferromagnetic component orders; susceptibility measurements indicate that this transition is due to an impurity and that there is no evidence of a magnetic transition in the herbertsmithite phase whose spins appear to remain dynamic down to the lowest temperatures studied.

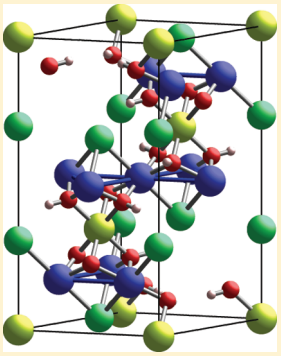

KEYWORDS: frustration, quantum, kagome, spin liquid, RVB, resonating valence bond

INTRODUCTION

Quantum spin liquids (QSLs) represent one of the great challenges in condensed matter research. Originally inspired by Anderson's proposal of the *resonating valence bond* (RVB) ground state,[1] a key reference for high temperature superconductivity, the search for QSLs has attracted many experimentalists and theorists. While the RVB state itself remains elusive, with only signatures being found,[2] the search has led to the discovery of several model magnets that fail to order into conventional ground states but instead display unconventional liquid-like behavior driven by exotic quantum effects. Much research into QSLs has focused on $S = 1/2$ magnets with the "highly frustrated" kagome and pyrochlore geometries, as these possess macroscopically degenerate ground states, capable of supporting unusual quantum behavior.[3−5] Excitement, and a resurgence of the field, was generated by the apparent lack of magnetic ordering in the mineral herbertsmithite, γ-$Cu_3Zn(OH)_6Cl_2$, a model kagome magnet.[6−9]

In herbertsmithite, the magnetic kagome system is formed by the segregation of Jahn−Teller active moment-bearing Cu^{2+} ($S = 1/2$) and diamagnetic Zn^{2+}.[10] The latter ions constitute triangular arrays that act as spacers between the kagome layers of its three-dimensional structure. Despite initial suggestions that herbertsmithite is a "perfect" model $S = 1/2$ kagome magnet,[9] further investigations have noted both extrinsic and intrinsic shortcomings of the samples. The proposed synthetic route has been shown by ^{17}O NMR,[11] powder neutron diffraction,[12] and heat capacity measurements[13] to introduce disorder between the Cu^{2+} and Zn^{2+} sites. As well as these defects, high-field EPR revealed herbertsmithite to possess significant antisymmetric exchange—the Dzyaloshinskii−Moriya interaction (DMI)[14−16]—an interaction that breaks the degeneracy of the ground state manifold and favors conventional magnetic order over a QSL.[5,17] These deviations from ideality make the lack of an ordered moment in herbertsmithite all the more remarkable. Subsequent theoretical work has gone on to show that the QSL states of kagome magnets can be surprisingly robust to deviations from the simple nearest-neighbor model.[18]

Since the discovery of herbertsmithite, a number of closely related transition metal hydroxy-chloride mineral phases have been identified. These new structures are inspiring new chemistry and opening the possibility of new model $S = 1/2$ kagome magnets, such as the recently discovered mineral kapellasite, α-$Cu_3Zn(OH)_6Cl_2$, and its isostructural and isomagnetic analogue, haydeeite α-$Cu_3Mg(OH)_6Cl_2$.[19−22] With an expanding number of model systems to study, it will become possible not only to separate the extrinsic properties of the individual systems from the intrinsic properties of their spin-fluid ground states but to understand how the QSLs respond to the different perturbations. One of the key references for understanding the properties of the QSL in herbertsmithite is the isomagnetic, Mg-exchanged analogue γ-$Cu_3Mg(OH)_6Cl_2$, hereafter referred to as Mg-herbertsmithite. For clarity of comparison, herbertsmithite itself, γ-$Cu_3Zn(OH)_6Cl_2$, will be referred to as Zn-herbertsmithite in the following discussion.

Zn-herbertsmithite is a member of the parent paratacamite family of minerals which has the general formula $Zn_x[Cu_{4-x}(OH)_6]Cl_2$, where $0 \le x \le 1$.[10] This series has been well studied

Received: November 3, 2010
Revised: February 22, 2011
Published: March 10, 2011

dx.doi.org/10.1021/cm103160q | *Chem. Mater.* 2011, 23, 1811–1817

Table 1. Crystallographic Parameters for Mg-Herbertsmithite, γ-$Cu_{4-x}Mg_x(OH)_6Cl_2$, Sample 2 at T = 295 K, Using X-Rays of λ = 0.412260 Å[a]

Wyckoff site	atom name	x	y	z	occupation
9*d*	Cu, Mg	1/3	1/6	1/6	0.955(3), 0.045(3)
3*a*	Mg, Cu	0	0	0	0.827(9), 0.173(9)
6*c*	Cl	0	0	0.30483(4)	1
18*h*	O	0.12778(6)	0.25557(12)	0.10396(6)	1
18*h*	H	0.2021(11)	0.4043(21)	0.0870(10)	1

[a] The refined lattice parameters are $a = b$ = 6.838861(11) Å and c = 14.021250(27) Å in the hexagonal setting of the space group $R\bar{3}m$. The final goodness-of-fit merit factor, χ^2, was 2.228.

with regard to quantum magnetism and features many properties that are still not fully understood, such as the nature of the phase transitions in the pyrochlore-like x = 0 end member, the mineral clinoatacamite.[23−28] Within the physics community "perfect" Zn-herbertsmithite has proved to be captivating. This is defined as having x = 1, which corresponds to 100% occupation of the kagome site by the S = 1/2 Cu^{2+}.[9] The similarity of the ionic radii of Mg^{2+} and Zn^{2+}[29] suggests that the flexibility of the flexibility of the paratacamite structure to a wide range of Zn/Cu ratios can also be expected to be true for the Mg analogues. This possibility has been supported by the recent report of members ranging from $0.33 \leq x \leq 0.75$.[30] Here, we present a study of the synthesis, crystal structures, and magnetic properties of Mg-herbertsmithite samples that are close to the idealized kagome structure, with compositions that lie in the range $0.93 \leq x \leq 0.98$.

SYNTHESIS

Mg-herbertsmithite can be synthesized following the reaction employed for the series of Zn-paratacamite, $Zn_x[Cu_{4-x}(OH)_6]Cl_2$, where $0.33 < x < 1$:[9]

$$3Cu_2(OH)_2CO_3 + 2MgCl_2 + 3H_2O \rightarrow 2Cu_3Mg(OH)_6Cl_2 + 3CO_2 \quad (1)$$

The reactions were carried out in 20 mL PTFE-lined steel hydrothermal bombs charged with 600 mg of finely ground basic copper carbonate (2.7 mmol), a ~2.667 mL aliquot of a 3 M magnesium chloride stock solution, and sufficient distilled water to make the solution up to 10 mL. The bomb was heated to 190 °C at a rate of 0.1 °C/min under autogenous pressure, left for 24 h, and cooled back to room temperature at 0.1 °C/min. Filtration of the resultant solution afforded green polycrystalline samples of Mg-herbertsmithite, characterized by laboratory powder X-ray diffraction. These were then washed with distilled water (3 × 20 mL) and acetone (3 × 20 mL) before drying (yield: 689 mg, 98.4%). This synthesis was repeated with a range of [$MgCl_2$] values between 0.5 and 4 M.

The use of solutions with concentrations below 0.7 M and above 3 M was found to give rise to CuO and haydeeite phase impurities, respectively. Studies using laboratory powder X-ray diffraction showed that $MgCl_2$ concentrations in the range 0.8−1.8 M yielded values of x closest to 1 and, so, to the most idealized structure. Samples **1**−**6** refer to preparations with 0.8, 1.0, 1.2, 1.4, 1.6, and 1.8 M $MgCl_2$ solutions, respectively.

Elemental analysis was performed on samples of ~10 mg dissolved in 10 mL of HNO_3 and made up to 100 mL with ultrapure water, using a Varian Vista Axial ICP-AES spectrometer.

Table 2. Comparison of Selected Refined Bond Lengths for Mg-Herbertsmithite, γ-$Cu_{4-x}Mg_x(OH)_6Cl_2$, with Those of Deuterated Zn-Herbertsmithite, γ-$Cu_3Zn(OD)_6Cl_2$[12]

	length (Å)	
bond	Mg-herbertsmithite	Zn-herbertsmithite[12]
$Cu-Cu_{intraplane}$	3.41943(5)	3.419
$Cu-Cu_{interplane}$	5.07360(8)	5.084
Cu−O(H/D)	1.9933(4)	1.985
Mg(Zn)−O(H/D)	2.1014(8)	2.109
O−H/D	0.954(13)	0.975
Cu−Cl	2.7659(4)	2.763

Table 3. A Comparison of Selected Refined Bond Angles of Mg-Herbertsmithite, γ-$Cu_3Mg(OH)_6Cl_2$, with Those of Deuterated Zn-Herbertsmithite[12]

	Angle (deg)	
bond	Mg-herbertsmithite	Zn-herbertsmithite[12]
Cu−O(H/D)−Cu	118.122(42)	118.89
Cu−O(H/D)−Mg(Zn)	96.644(24)	96.82
Cu−O−H/D	111.70(36)	114.88

ANALYSIS OF THE CRYSTAL STRUCTURES

High resolution synchrotron X-ray diffractograms were collected, using beamline 11-BM of the Advanced Photon Source,[31] from samples **1**−**6**. Structural details, obtained using the Rietveld refinement program TOPAS,[32] showed only minor variations in the structure across the series (see Figure 1; complete refined structures and comparisons given in the Supporting Information). Selected structural information for one of the samples (**2**) is presented in Tables 1, 2, and 3. For comparison, Tables 2 and 3 also contain structural information for deuterated Zn-herbertsmithite, refined using high-resolution powder neutron diffraction data.[12]

Just as in Zn-herbertsmithite, the structure is composed of a pyrochlore-like lattice of metal ions where Cu^{2+} preferentially resides on the Jahn−Teller distorted kagome (9*d*) sites, leaving occupation of the interplanar triangular (3*a*) sites by Mg^{2+}. The kagome lattice, of nominally Cu^{2+}, is held together on one face by three bridging μ_3-hydroxy groups that are further bound to the triangular Mg^{2+} sites. The other face of each kagome triangle is capped by a μ_3-chloride ion, hydrogen bonded to the hydroxy groups of the neighboring plane. Any exchanged Cu^{2+} ions present on the triangular (3*a*) site allow for the possibility of

dx.doi.org/10.1021/cm103160q |*Chem. Mater.* 2011, 23, 1811–1817

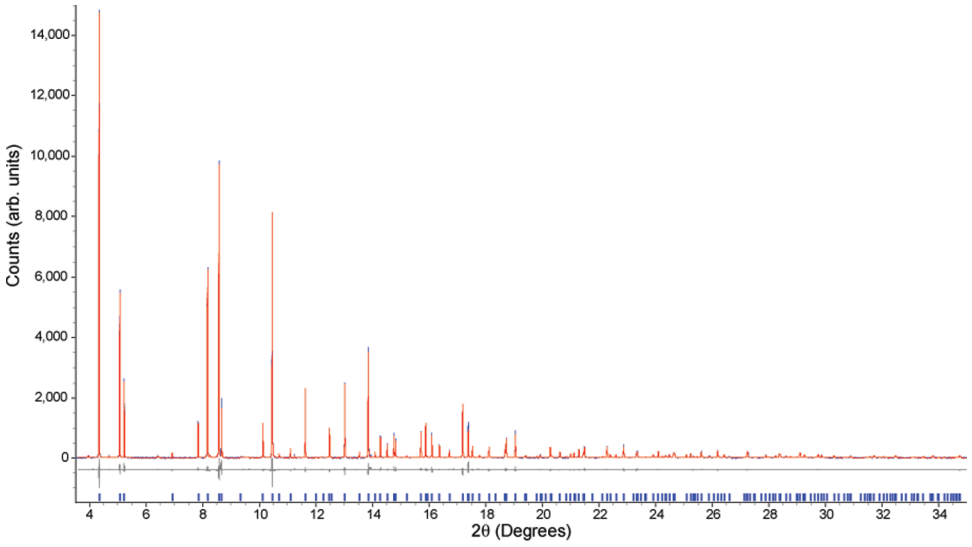

Figure 1. Rietveld refinement using TOPAS of synchrotron powder X-ray diffraction data of Mg-herbertsmithite, γ-$Cu_{4-x}Mg_x(OH)_6Cl_2$ sample **2**, at T = 295 K and using X-rays of wavelength λ = 0.412260 Å. The final goodness-of-fit merit factor, χ^2, was 2.228.

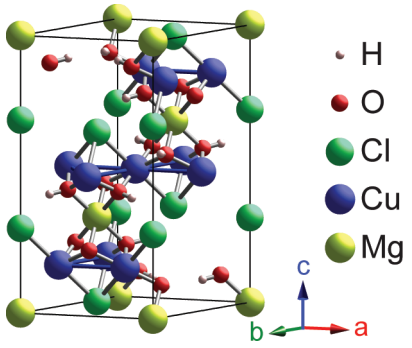

Figure 2. The refined crystal structure of Mg-herbertsmithite, γ-$Cu_3Zn(OH)_6Cl_2$, showing the pyrochlore-like lattice of metal sites, with preferential occupation of Mg^{2+} at the triangular-antiprism (3*a*) sites and Cu^{2+} at the kagome (9*d*) sites.

interplane coupling in the herbertsmithite structure. This three-dimensionality is notably different from the respective Zn and Mg polymorphs kapellasite and haydeeite, where the kagome planes are only weakly bound to neighboring planes through O—H···Cl hydrogen bonding.[19,20]

As can be seen in Tables 2 and 3 and Figure 2, the structure of Mg-herbertsmithite varies very little from that of Zn-herbertsmithite.[12] This is unsurprising as the differences between the ionic radii of Zn^{2+}, Cu^{2+}, and Mg^{2+} are small (0.74, 0.73, and 0.72 Å, respectively[29]), and both Zn^{2+} and Mg^{2+} ions favor similar isotropic coordination environments. The substitution of Mg^{2+} for Zn^{2+} is seen to have only a small effect on the intraplane Cu—Cu distances; the geometries of the underlying kagome lattices of these herbertsmithites are very similar. There is, however, a small contraction of the interplane Cu—Cu distance (~0.2%) and the *c* axis, as would be expected upon substitution of the Zn^{2+} with smaller Mg^{2+} on the interplanar triangular (3*a*) site.

Of particular importance for the magnetism is the Cu—O—Cu superexchange, characterized by the Cu—O bond length and Cu—O—Cu bond angle. The Cu—O bond lengths are nearly the same in the Zn- and Mg-herbertsmithites, but a slightly smaller Cu—O—Cu bond angle is seen in the Mg analogue. As this value decreases toward 90°, the sign of the superexchange is expected to crossover from antiferromagnetic to ferromagnetic, but the difference between the angles for these two materials is so small (0.77°) that such a crossover is unlikely. Another important structural comparison is the O—H bond length, as this has been shown by DFT calculations to give an indication of the hybridization of the μ_3-hydroxy groups that mediates the superexchange, in related materials.[33,34] Again, the difference in this bond length between the two materials is so small, ~0.021 Å, that the oxygen hybridization and their associated exchange are expected to be the same.

The sizable differences in the atomic scattering factors of Cu^{2+} and Mg^{2+} allow the metal site occupancies to be reliably refined using X-ray diffraction. With only the assumption that the total site occupation was unity, the refinements were found to be stable but not to give unique solutions. Additional constraints were therefore applied to fix the total Mg—Cu ratios to be the same as those determined by ICP-AES elemental analysis (Figure 3a). Refined occupancies of the kagome (9*d*) and intralayer triangular (3*a*) sites are shown in (Figure 3b). Just as in Zn-herbertsmithite,[12] the Jahn—Teller active Cu^{2+} ions display a preference for the distorted octahedron of the kagome (9*d*) sites over the symmetric coordination of the triangular antiprism sites (3*a*) that separate the kagome planes.

The crystallographic refinements indicate that the kagome sites (9*d*) are occupied by ~95% Cu^{2+}, with a small increase in the dilution of the kagome sites by Mg^{2+} across samples **1**—**6**, from 4.39(4)% to 5.45(4)%. Quite different behavior is seen for the refined occupancy of the triangular (3*a*) site: this shows little variation across the series; the occupation by Cu^{2+} has an average value of 18.3(8)%. This occupation value of the triangular (3*a*) site by the magnetic ions is important when considering the dimensionality of the magnetism in the herbertsmithites, as it is the presence of Cu^{2+} on this site that leads to coupling between the kagome planes and destroys the local two-dimensionality. We note that our refined diamagnetic occupation of the triangular (3*a*) site in Mg-herbertsmithite is within the range reported for the isomagnetic Zn-herbertsmithite.[12]

dx.doi.org/10.1021/cm103160q |*Chem. Mater.* 2011, 23, 1811–1817

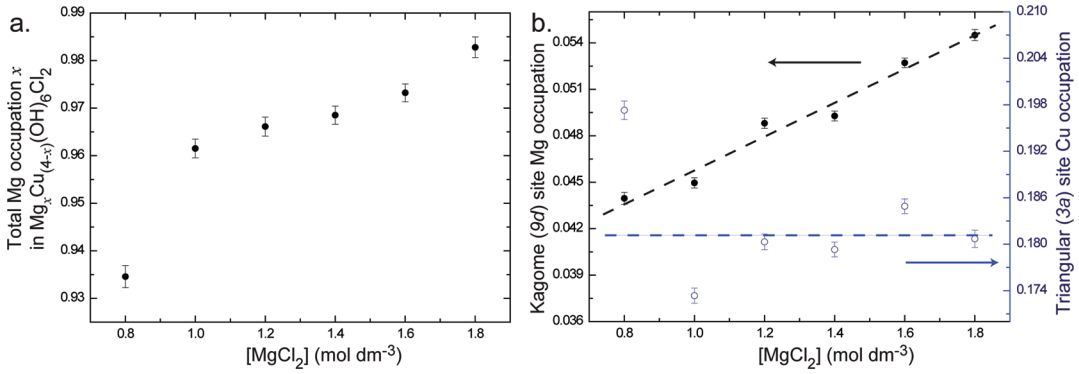

Figure 3. (a) Total refined Mg occupation, x, in the formula γ-$Cu_{4-x}Mg_x(OH)_6Cl_2$, showing a slightly lower than idealized $x = 1$ occupation of diamagnetic Mg^{2+} onto the $S = 1/2$ Cu^{2+} pyrochlore-like lattice, with a trend of increasing x as the $[MgCl_2]$ concentration is increased toward the $x = 1$ idealized stoichiometry. (b) Refined Mg^{2+} occupation on the kagome ($9d$) site (left) and Cu^{2+} occupation of the triangular ($3a$) site (right). A positive trend can be seen in diamagnetic dilution of the kagome lattice upon increasing the solution concentration. Conversely, there is no systematic change, upon increasing solution concentration, in the Cu^{2+} occupation of the triangular ($3a$) site.

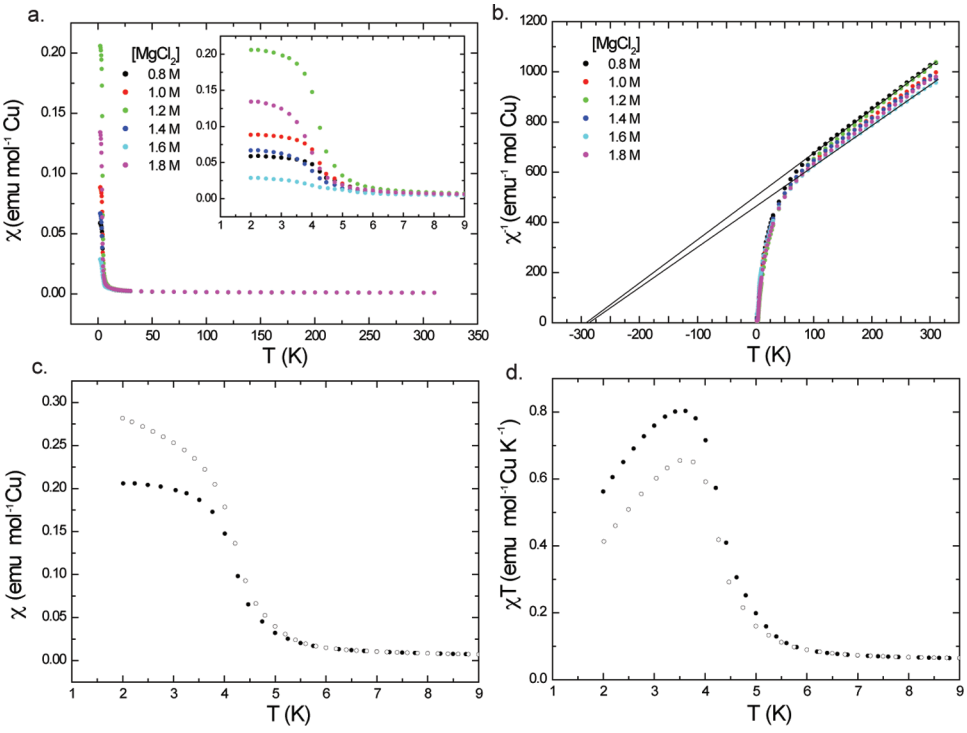

Figure 4. (a) Zero-field-cooled magnetic susceptibility of samples **1**−**6** measured in a 100 Oe field. A rapid increase is seen below $T_C = 4-5$ K, suggestive of a ferromagnetic transition. Inset: a blow-up of the low T region, where the saturation value does not appear to follow a trend across the series of samples. (b) Inverse susceptibility, showing a large-negative intercept of Curie−Weiss fits to the high temperature region ($100 > T > 300$ K), with all samples giving similar values of $\theta_W = -284(23)$ K. (c) Zero-field-cooled (●) and field-cooled (○) susceptibility for sample **3** showing bifurcation during the transition at $T_C = 4-5$ K. (d) A plot of χT against the temperature for sample **3** shows a downturn below the ferromagnetic transition that is indicative of competing antiferromagnetic and ferromagnetic contributions to the averaged response.

These results contrast with those recently reported from laboratory X-ray refinements of small single crystals of Mg-paratacamites, γ-$Cu_{4-x}Mg_x(OH)_6Cl_2$, with total Mg occupancies that range from $x = 0.33$ to 0.75.[30] For the three samples of this series, only variation in the Mg^{2+} occupation of the triangular ($3a$) site was seen; the kagome ($9d$) site remained completely occupied by $S = 1/2$ Cu^{2+} ions for all values of $[MgCl_2]$. The difference in the occupations of our powder samples of Mg-herbertsmithite and the single crystals of the Mg-paratacamites is likely to be a consequence of the dissimilar reaction conditions: our powder samples were prepared over a 48 h period, while the single crystals were grown over 45 weeks.[30] The latter would therefore be expected to display occupancies that are closer to the thermodynamic limit.

MAGNETIC SUSCEPTIBILITY

Zero-field-cooled (ZFC) and field-cooled (FC) magnetic susceptibility (χ) measurements were taken in a field of 100 Oe

dx.doi.org/10.1021/cm103160q |*Chem. Mater.* 2011, 23, 1811–1817

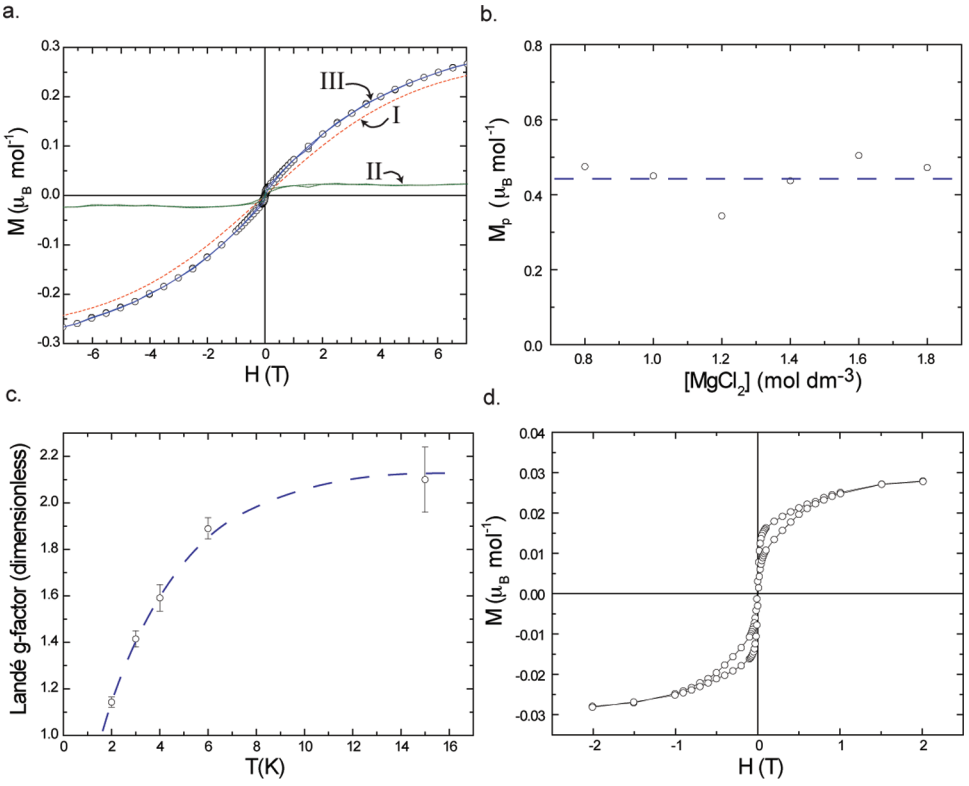

Figure 5. (a) Magnetization against field over temperature sweep at 2.0 K showing paramagnetic-like behavior (○) for sample **1**. (I) Fit to the $S = 1/2$ Brillouin function, (II) the extracted ferromagnetic component, (III) paramagnetic + ferromagnetic components showing excellent fit to the data. (b) The saturation magnetization of the paramagnetic component, M_p, as a function of $[MgCl_2]$ for samples **1**−**6** at $T = 2$ K with a guide to the eye in blue, showing little composition dependence. (c) The fitted Landé g-factor as a function of temperature, for sample **1**, showing the buildup of correlations below $T = 6$ K, with a guide for the eye in blue indicating a high temperature limit of $g_L \sim 2.1$. (d) The extracted ferromagnetic hysteresis for sample **1**, at $T = 2$ K, believed to be caused by an impurity phase.

with a Quantum Design MPMS-7 SQUID magnetometer (Figure 4). Fits of the linear region of the inverse susceptibility, over the temperature range $100 < T < 300$ K, yielded large negative Weiss temperatures of $\theta_W \simeq -284(23)$ K, a value that is close to those that have been found in Zn-herbertsmithite, $\theta_W = -301$ K (Curie−Weiss fits for the entire series are given in the Supporting Information).[9] On cooling below $T \sim 100$ K, curvature develops in the $\chi^{-1}(T)$, indicating the formation of spin−spin correlations; such behavior is a familiar characteristic of both classical and quantum kagome systems.[9,19,20,35−38] It is only upon cooling to far lower temperatures that a transition is observed as a rapid increase in χ below $T_C \simeq 4-5$ K that is accompanied by bifurcation of ZFC and FC data. If this transition was from the herbertsmithite phase, its strong suppression, $|\sim\theta_W|/T_C \sim 66$, would indicate that Mg-herbertsmithite is indeed a highly frustrated magnet. However, the decrease in χT vs T below 4 K indicates that the ferromagnetic transition involves a significant antiferromagnetic component, a juxtaposition that raises the question of whether the two responses are from the same phase.

In an effort to determine the nature of the ferromagnetic component, measurements of the magnetization, M, were recorded for each of the samples in fields, H, between −7 and 7 T at several temperatures above and below the $T_C \sim 4-5$ K transition. All data exhibit a typical paramagnetic-like response, with the development of a ferromagnetic response below $T_C \sim 4-5$ K. The paramagnetic response was fitted with an $S = 1/2$ Brillouin function[39] and allowed extraction of a distinctly separate, saturating, ferromagnetic hysteresis loop (Figure 5a). (Full details of the fitting procedure and the resultant fits for all samples can be found in the Supporting Information.) The fit yielded a saturation magnetization of the paramagnetic component, M_p, at 2 K of $\sim 0.45\ \mu_B$ mol^{-1} (Figure 5b), well below the $3\ \mu_B$ mol^{-1} expected for the formula unit $Cu_3Mg(OH)_6Cl_2$ if all Cu^{2+} spins were contributing. At high temperatures ($T \geq 15$ K), the fitted g-factor tends toward $g_L \sim 2.1$, a value similar to those seen in Zn-herbertsmithite,[13,16] but upon cooling below 6 K, the form of the Brillouin function changes and the fitted values of g_L reduce rapidly (Figure 5c), indicating that below this transition the paramagnetic-like spins couple more strongly to the neighboring spins. Subtraction of the Brillouin function from the field-dependence of the magnetization reveals a weak hysteresis that has a saturation value of $\sim 2.5 \times 10^{-2}\ \mu_B$ mol^{-1} and a coercive field of ~100 G at $T = 2$ K (Figure 5d). This saturation value indicates that the ferromagnetic component represents only ~1−2% of all Cu^{2+} in the sample. The apparently random variation in the size of the saturated ferromagnetic moment (see Supporting Information) supports the hypothesis that it is from varying amounts of an impurity rather than changes in the crystal structure, as the crystallographic refinements indicate that the latter correlate well with the synthesis conditions. The continued presence of the Brillouin function characteristic of paramagnetic-like spins below the ferromagnetic transition requires that the two responses have different origins and is also compatible with the presence of a small amount of a ferromagnetic impurity. The constancy of the

dx.doi.org/10.1021/cm103160q |*Chem. Mater.* 2011, 23, 1811–1817

ferromagnetic ordering temperature across the Mg-herbertsmithite (and paratacamite[30]) series suggests that the same impurity is involved in all these systems and explains why the samples of the Mg-paratacamite phases with $x = 0.33-0.75$, which feature far greater occupation of the triangular Mg^{2+} site by Cu^{2+}, also have transitions close to those found in Mg-herbertsmithite, $T_C \sim 4-5$ K *despite* featuring a large variation in Weiss temperatures.[30]

Looking now at the fits to the Brillouin function, a comparison with Zn-herbertsmithite[13] suggests that spins on the interplane triangular layer will only weakly couple with the spins of the kagome layer to create a paramagnetic-like component, M_P. This appears not to be the case as the observed size of M_p is close to 2.5 times that which would be expected if the spins involved were solely due to *free* Cu^{2+} on the triangular sites. It follows that if the Cu^{2+} ions on the triangular site are responsible, then they are ferromagnetically coupled to some of the spins in the neighboring kagome layers to create superparamagnetic clusters of spins. In the Mg-herbertsmithites presented in this study, there are few such clusters, but larger quantities of Cu^{2+} on the triangular site will correspondingly lead to a lessening of the antiferromagnetic mean field and a reduction in the magnitude of the Weiss temperature, a behavior that has been seen in the Mg-paratacamites.[30] The reduction in g_L at low temperatures indicates that these clusters cannot be considered as free. Attempts were made to fit the paramagnetic-like curvature with an alternative modified Brillouin function,[40] holding the Landé g-factor at that of a free electron while replacing the temperature with an effective temperature, $T_{eff} = T - T_W$. In all cases, the variable T_W (comparable to a Weiss temperature θ_W) refined to ~ -1.5 K, suggesting that interactions between these superparamagnetic clusters are weak and antiferromagnetic, in agreement with the reduction in g_L when the normal Brillouin function is used. Extension of the clusters beyond the spins of the triangular site requires that they are coupled to the spins of the kagome lattice. The coupling between spins on the triangular sites is far weaker than the value of $\theta_W = -284(23)$ K, observed from the high-temperature bulk susceptibility that involves all of the spins within the structure. The retention of Brillouin-like behavior at all temperatures indicates that this coupling stiffens the fluctuations of the superparamagnetic clusters but does not freeze them—a behavior that requires the kagome spins to remain dynamic at low temperatures and for these to be in a quantum spin liquid state.

In conclusion, we present crystallographic and magnetic studies of the new model kagome magnet Mg-herbertsmithite, γ-$Cu_{4-x}Mg_x(OH)_6Cl_2$, in the range $0.93 \leq x \leq 0.98$. A small ferromagnetic ordering is observed at $T_C \sim 4-5$ K in all samples that is assigned to an impurity phase. The Mg-herbertsmithite phases show no evidence of magnetic transitions down to 1.8 K, and low-temperature magnetometry measurements suggest the formation of a quantum spin liquid (QSL).

■ ASSOCIATED CONTENT

Supporting Information. An analysis of the crystal structures and additional information regarding magnetometry are provided. This material is available free of charge via the Internet at http://pubs.acs.org.

■ AUTHOR INFORMATION

Corresponding Author

*E-mail: a.s.wills@ucl.ac.uk.

Present Addresses

‡Edinburgh University, Department of Chemistry, The King's Buildings, West Mains Road, Edinburgh, EH9 3JJ

■ ACKNOWLEDGMENT

The authors would like to thank the Royal Society and the EPSRC, grant EP/C534654, for funding. Use of the Advanced Photon Source at Argonne National Laboratory was supported by the U.S. Department of Energy, Office of Science, Office of Basic Energy Sciences, under Contract No. DE-AC02-06CH11357. Thanks also go to Prof. Phillipe Mendels and Dr. Fabrice Bert for insightful discussions and Diana Dragoe for performing the ICP-AES analysis.

■ REFERENCES

(1) Anderson, P. W.; Baskaran, G.; Zou, Z.; Hsu, T. *Phys. Rev. Lett.* **1987**, *58*, 2790.
(2) Rinnow, H. M.; McMorrow, D. F.; Coldea, R.; et al. *Phys. Rev. Lett.* **2001**, *87*, 037202.
(3) Greedan, J. E. *J. Alloys Compd.* **2006**, *408*, 444.
(4) Sciffer, P.; Ramirez, A. P.; Franklin, K. N.; Cheong, S. W. *Phys. Rev. Lett.* **1996**, *77*, 2085.
(5) Ballou, R.; Canals, B.; Elhajal, M.; Lacroix, C.; Wills, A. S. *J. Magn. Magn. Mater.* **2003**, *262*, 465.
(6) Bert, F.; Nakamae, S.; Ladieu, F.; L'Hote, D.; Bonville, P.; Duc, F.; Trombe, J. C.; Mendels, P. *Phys. Rev. B* **2007**, *76*, 132411.
(7) Helton, J. S.; Matan, K.; Shores, M. P.; Nytko, E. A.; Bartlett, B. M.; Yoshida, Y.; Takano, Y.; Suslov, A.; Qiu, Y.; Chung, J. H.; Nocera, D. G.; Lee, Y. S. *Phys. Rev. Lett.* **2007**, *98*, 107204.
(8) Mendels, P.; Bert, F.; de Vries, M. A.; Olariu, A.; Harrison, A.; Duc, F.; Trombe, J. C.; Lord, J. S.; Amato, A.; Baines, C. *Phys. Rev. Lett.* **2007**, *98*, 077204.
(9) Shores, M. P.; Nytko, E. A.; Bartlett, B. M.; Nocera, D. G. *J. Am. Chem. Soc.* **2005**, *127*, 13462.
(10) Braithwaite, R. S.; Mereiter, K.; Paar, W. H.; Clark, A. M. *Mineral. Mag.* **2004**, *68*, 527.
(11) Olariu, A.; Mendels, P.; Bert, F.; Duc, F.; Trombe, J. C.; de Vries, M. A.; Harrison, A. *Phys. Rev. Lett.* **2008**, *100*, 087202.
(12) Lee, S. H.; Kikuchi, H.; Qiu, Y.; Lake, B.; Huang, Q.; Habicht, K.; Kiefer, K. *Nat. Mater.* **2007**, *6*, 853.
(13) de Vries, M. A.; Stewart, J. R.; Deen, P. P.; Piatek, J. O.; Nilsen, G. J.; Ronnow, H. M.; Harrison, A. *Phys. Rev. Lett.* **2009**, *103*, 237201.
(14) Rigol, M.; Singh, R. R. P. *Phys. Rev. B* **2007**, *76*, 180407.
(15) Rigol, M.; Singh, R. R. P. *Phys. Rev. Lett.* **2007**, *98*, 207204.
(16) Zorko, A.; Nellutla, S.; van Tol, J.; Brunel, L. C.; Bert, F.; Duc, F.; Trombe, J. C.; de Vries, M. A.; Harrison, A.; Mendels, P. *Phys. Rev. Lett.* **2008**, *101*, 026405.
(17) Elhajal, M.; Canals, B.; Lacroix, C. *Phys. Rev. B* **2002**, *66*, 014422.
(18) Cepas, O.; Fong, C. M.; Leung, P. W.; Lhuillier, C. *Phys. Rev. B* **2008**, *78*, 140405.
(19) Colman, R. H.; Ritter, C.; Wills, A. S. *Chem. Mater.* **2008**, *20*, 6897–6899.
(20) Colman, R. H.; Sinclair, A.; Wills, A. S. *Chem. Mater.* **2010**, *22*, 5774–5779.
(21) Schluter, J.; Malcherek, T. *N. Jb. Miner. Abh.* **2007**, *184*, 39.
(22) Krause, W.; Bernhardt, H. J.; Braithwaite, R. S. W.; Kolitsch, U.; Pritchard, R. *Mineral. Mag.* **2006**, *70*, 329.
(23) Wills, A. S.; Raymond, S; Henry, J.-Y. *J Magn. Magn. Mater.* **2004**, *272*, 850–851.
(24) Wills, A. S.; Henry, J. Y. *J. Phys. Condens. Mater.* **2008**, *20*, 472206.
(25) Wills, A. S.; Perring, T. G.; Raymond, S.; Fåk, B.; Henry, J. Y. *J. Phys.: Conf. Ser.* **2009**, *145*, 012056.

(26) Zheng, X. G.; Kawae, T.; Kashitani, Y.; Li, C.; Tateiwa, N.; Takeda, K.; Yamada, H.; Xu, C.; Ren, Y. *Phys. Rev. B* **2005**, *71*, 052409.
(27) Zheng, X., G.; Mori, T.; Nishiyama, K.; Higemoto, W.; Yamada, H.; Nishikubo, K.; Xu, C. *Phys. Rev. B* **2005**, *71*, 174404.
(28) Zheng, X., G.; Kubozono, H.; Nishiyama, K.; Higemoto, W.; Kawae, T.; Koda, A.; Xu, C. *Phys. Rev. Lett.* **2005**, *96*, 057201.
(29) Shannon, R. D. *Acta Crystallogr.* **1976**, *A32*, 751.
(30) Chu, S.; McQueen, T. M.; Chisnell, R.; Freedman, D. E.; Muller, P.; Lee, Y. S.; Nocera, D. G. *J. Am. Chem. Soc.* **2010**, *132*, 5570.
(31) Wang, J.; Toby, B. H.; Lee, P. L.; et al. *Rev. Sci. Instrum.* **2008**, *79*, 085105.
(32) *TOPAS*; Bruker AXS GmbH: Karlsruhe, Germany.
(33) Janson, O.; Richter, J.; Rosner, H. *Phys. Rev. Lett.* **2008**, *101*, 106403.
(34) Janson, O.; Richter, J.; Rosner, H. *J. Phys. Conf. Ser.* **2008**, *145*, 012008.
(35) Obradors, X.; Labarta, A.; Isalgue, A.; Tejada, J.; Rodriguez, J.; Pernet, M. *State Commun.* **1988**, *65*, 189.
(36) Wills, A. S.; Harrison, A. *J. Chem. Soc., Faraday. Trans.* **1996**, *92*, 2161–2166.
(37) Wills, A. S.; Oakley, G. S.; Visser, D.; Frunzke, J.; Harrison, A.; Andersen, K. H. *Phys. Rev. B* **2001**, *64*, 094436.
(38) Oakley, G. S.; Visser, D.; Frunzke, J.; Andersen, K. H.; Wills, A. S.; Harrison, A. *Physica B* **1999**, *267*, 142–144.
(39) Kittel, C. *Introduction to solid state physics*, 7th ed.; John Wiley & Sons, Inc.: New York, 2004; pp 417−422.
(40) Gaj, J. A.; Planel, R.; Fishman, G. *Solid State Commun.* **1979**, *29*, 435.